Estimating Speed Using a Side-Looking Single-Radar Vehicle Detector

Shyr-Long Jeng, Wei-Hua Chieng, and Hsiang-Pin Lu

***Abstract*—This paper presents a side-looking single-beam microwave vehicle detector (VD) system for estimation of per-vehicle speed and length. The proposed VD system is equipped with a 2-D range Doppler frequency-modulated continuous-wave (FMCW) radar using a squint angle. The associated Fourier processor uses an inverse synthetic aperture radar (ISAR) algorithm to extract range and speed data for each vehicle using a single-beam FMCW radar. The simulation and experimental results show accurate estimations of vehicle speed and length. The measurement errors of speed and length were approximately ± 4 km/h and ± 1 m, respectively. The proposed method has excellent detection capability for small moving targets, such as bikes and pedestrians, at speeds down to 5 km/h. A commercial 10.6-GHz radar with signal processing modifications was used in the experiments.**

***Index Terms*—Frequency-modulated continuous wave (FMCW), intelligent transportation system (ITS), synthetic aperture radar (SAR), vehicle detector (VD).**

I. Introduction

VEHICLE detectors (VDs) are widely used to gather traffic information in an intelligent transportation system (ITS). The objective of a VD is to obtain traffic information, such as the speed and length of vehicles passing on a road. A wide range of sensor technologies are available for VDs, such as inductive loops, video, ultrasonic detectors, and microwave detectors. The advantage of radar-based detectors is that they are a mature technology because of past military applications. Radar-based detectors are unintrusive and can operate day or night in any weather conditions. A frequency-modulated continuous-wave (FMCW) radar is widely used for traffic data collection. It transmits a continuous-wave (CW) signal and compares the frequency difference between the transmitted and reflected signals to estimate the vehicle range and its speed.

The installation methods of radar-based detectors can be classified as forward-looking and side-looking (or roadside). Forward-looking detectors have an illuminative direction parallel to the direction of traffic and are applied only to a single lane [1]. Conversely, Fig. 1 shows that side-looking radar detectors illuminate the direction perpendicular to traffic. A single-radar detector in a side-looking configuration can cover multiple lanes if it is properly placed and if appropriate signal processing techniques are used. In this case, microwave sensors can replace a large number of loops, which are usually installed in the travel lanes. Perpendicular side-looking installation is the most popular approach for current ITS applications. The working theory of a side-looking VD is the same as that of a single loop in each lane. When the vehicle length and vehicle speed are uncorrelated, vehicle speed v and vehicle length l are related by

$$v = \frac{l}{t}. \tag{1}$$

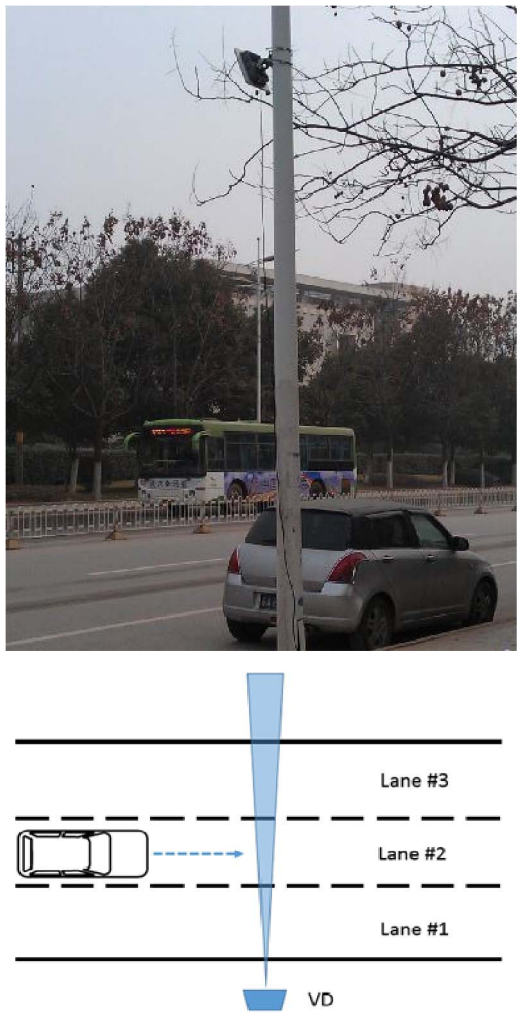

Fig. 1. Conventional side-looking vehicle detection systems.

Manuscript received May 17, 2013; revised July 9, 2013 and September 17, 2013; accepted September 19, 2013. Date of publication October 17, 2013; date of current version March 28, 2014. This work was supported by the National Science Council of Taiwan under Contract NSC 101-3113-E-009-006. The Associate Editor for this paper was F. Zhu.

S.-L. Jeng is with the Department of Electrical and Electronic Engineering, Ta Hwa University of Science and Technology, Hsinchu 307, Taiwan (e-mail: aetsl@tust.edu.tw).

W.-H. Chieng and H.-P. Lu are with the Department of Mechanical Engineering, National Chiao Tung University, Hsinchu 300, Taiwan (e-mail: whc@cc.nctu.edu.tw; champ.lu@gmail.com).

Color versions of one or more of the figures in this paper are available online at http://ieeexplore.ieee.org.

Digital Object Identifier 10.1109/TITS.2013.2283528

These parameters cannot be independently measured in a single loop. A single loop can only detect dwell time t. Vehicle length l is typically set to a constant value, and (1) is used to estimate speed from single-loop measurements. However, this approach does not consider varying vehicle lengths. During a low flow, a long vehicle can skew statistical data because it requires more time to pass the detector. Many studies [2]–[4] have addressed this problem.

Most side-looking radars can measure only the dwell time of a vehicle passing through the radar sensing zone. A single-beam radar served as a single induced loop to estimate speed based on the dwell time. Although dual-radar detectors can provide more accurate speeds and vehicle classifications by measuring the time difference between two radar beams, they encounter a number of problems. First, they require a highly precise installation to ensure perpendicularity to the direction of traffic; otherwise, matching the detected signals between two radars is difficult. The second problem is that the performance can be inhibited when one of the radar signals is blocked by nearby vehicles in traffic jam scenarios.

The conventional installation of a side-looking radar does not use the advantage of detecting the Doppler effect of microwave detectors because the returned Doppler frequency generated by the vehicle is weak. Prior studies [5], [6] have detected the weak Doppler shift for measuring real-time speed by using wide beam antennas. The disadvantage of this approach is degradation in range accuracy. Many other studies [7], [8] have used various waveforms and frequencies to obtain range and speed information. Because of the weak Doppler effect, the perpendicular side-looking VD cannot apply the typical FMCW speed detection method by comparing beat frequencies of up and down sweeps [9] or the displacement difference [10]. Therefore, it is crucial to develop an appropriate method with a narrow-beam single-radar detector to provide accurate range, speed, and vehicle classification estimates.

This paper proposes a novel radar system to detect multiple vehicles in multiple lanes. The following section presents the associated FMCW radar measurement scheme and the associated 2-D range Doppler FMCW radar Fourier processing method. The range and Doppler frequency were obtained using the 2-D fast Fourier transform (FFT) technique [11] widely used in inverse synthetic aperture radar (ISAR) signal processing [12]–[15]. Vehicle detection was performed by using a high-speed digital signal processor (DSP) and a 10.6-GHz FMCW front end. This paper also presents an algorithm to measure the speed and vehicle length by using a fixed single-radar module.

The remainder of this paper is organized as follows. Section II briefly describes the derivation of the proposed method and Section III presents the measurement results to illustrate the capability of the proposed method. Finally, Section IV concludes the study.

II. Proposed Method

Fig. 2 shows an FMCW-based VD installed on a roadside with a squint angle. In this configuration, the Doppler frequency returned from the moving vehicle is enhanced compared with that from the perpendicular VD. Fig. 3 shows a typical FMCW

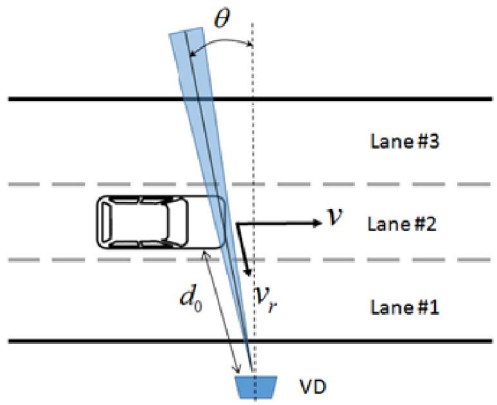

Fig. 2. Proposed VD installation.

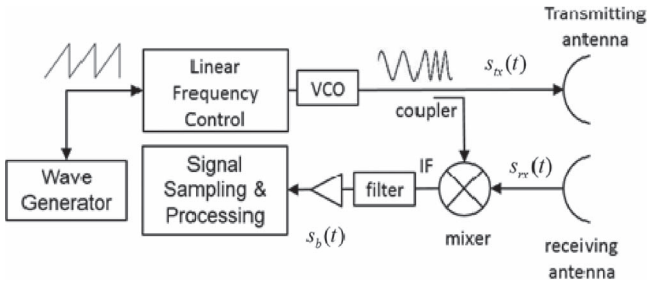

Fig. 3. Typical FMCW-based radar architecture.

radar setup. For a side-looking FMCW VD, the range data retrieved from up and down sweeps are almost the same except for a little phase difference. In addition, a triangular waveform doubles the time span on a sweep; it reduces the pulse repetition frequency (PRF) and downgrades the Doppler frequency detection. Therefore, a sawtooth waveform is used instead of a triangular waveform. The CW signal is modulated in the frequency to produce a linear chirp, which radiates toward a target through an antenna. The echo $s_{rx}(t)$ received $\tau(t)$ seconds later is mixed with a portion of the continuous transmitted signal $s_{tx}(t)$ to produce a beat signal at frequency $s_b(t)$, which is proportional to the roundtrip time-of-flight (RTOF) $\tau(t)$ between the radar and the target.

The transmitted signal can be expressed as

$$s_{tx}(t) = A_{tx}\cos\left(\phi_{tx}(t)\right) \tag{2}$$

where the instantaneous phase term is

$$\phi_{tx}(t) = \omega_{c0}t + \frac{\alpha}{2}t^2 + \phi_{tx0}.$$

The carrier frequency in which the modulation starts is denoted by $\omega_{c0} = 2\pi f_{c0}$. Sweep rate $\alpha = 2\pi(B/T)$ is equal to the quotient of radar signal sweep bandwidth B and sweep duration T. t is the time variable in the range $0 < t < T$. Signal $s_{rx}(t)$, which is reflected by the target and received by the radar, is a replica of the transmitted signal; however, it is delayed by the RTOF. The signal received from the target is delayed and attenuated, i.e.,

$$s_{rx}(t) = A_{rx}s_{tx}\left(t - \tau(t)\right). \tag{3}$$

The received and transmitted signals, i.e., $s_{rx}(t)$ and $s_{tx}(t)$, are multiplied in the mixer. A low-pass filter is used to suppress the signal components located at the double carrier frequency. By solving the multiplication and considering (2) and (3), a beat signal was obtained as

$$s_b(t) = A_b \cos\left(\omega_{c0}\tau(t) + \alpha\tau(t)t - \frac{1}{2}\alpha\tau(t)^2\right). \quad (4)$$

Consider a target located at distance d at time $t = 0$ and moving at speed v. The target reflects the FMCW signal transmitted by the radar unit. Vehicle distance $d(t + kT_r)$ is defined as the range from the sensor to the vehicle at the kth sweep. $d(t + kT_r)$ is derived by

$$d(t + kT_r) = d_0 + v_r \cdot (t + kT_r), \qquad k = 0, 1, 2, \ldots, N-1$$

where v_r denotes the radial component of the vehicle speed at squint angle θ. T_r denotes the pulse repetition interval (PRI).

During NT_r, the coherent processing interval (CPI), the speed is assumed to be constant, and the RTOF $\tau(t + kT_r)$ between the radar and the target is defined as

$$\begin{aligned}\tau(t + kT_r) &\equiv \frac{2d(t + kT_r)}{c} \\ &= \frac{2}{c}\left(d_0 + v_r \cdot (t + kT_r)\right) \\ &= \tau_0 + 2\frac{v_r}{c}(t + kT_r) \end{aligned} \quad (5)$$

where τ_0 is the RTOF when the vehicle is at the initial range d_0. Replacing $\tau(t)$ in (4) with (5) derives a 2-D beat signal, i.e.,

$$s_b(t, kT_r) = A_b \cos(\phi_b) \quad (6)$$

where

$$\begin{aligned}&\phi_b(t, kT_r) \\ &= \omega_{c0}\tau(t + kT_r) + \alpha\tau(t + kT_r)t - \frac{1}{2}\alpha\tau(t + kT_r)^2 \\ &= \omega_{c0}\tau_0 + 2\omega_{c0}\frac{v_r}{c}(t + kT_r) + \alpha\tau_0 t + 2\alpha\frac{v_r}{c}(t + kT_r)t \\ &\quad - \frac{1}{2}\alpha\left[\tau_0^2 + 4\tau_0\frac{v_r}{c}(t + kT_r) + 4\left(\frac{v_r}{c}\right)^2(t + kT_r)^2\right] \\ &= \omega_{c0}\tau_0 + \left(2\omega_{c0}\frac{v_r}{c} + \alpha\tau_0 - 2\alpha\tau_0\frac{v_r}{c}\right)t \\ &\quad + \left(2\omega_{c0}\frac{v_r}{c} - 2\alpha\tau_0\frac{v_r}{c}\right)kT_r - \frac{1}{2}\alpha\tau_0^2 \\ &\quad + 2\alpha\frac{v_r}{c}\left(1 - \frac{v_r}{c}\right)t^2 + 2\alpha\frac{v_r}{c}\left(1 - \frac{v_r}{c}\right)tkT_r \\ &\quad - 2\alpha\left(\frac{v_r}{c}\right)^2(kT_r)^2. \end{aligned}$$

Without a loss of generality, this discussion assumes $(v_r/c) \ll 1$, and the term $2\alpha(v_r/c)^2(kT_r)^2$ is ignored. Equation (6) can be rewritten as

$$\begin{aligned}&\phi_b(t, kT_r) \\ &= \left(\omega_{c0}\frac{2v_r}{c} + \alpha\tau_0\right)t + \left(\omega_{c0}\frac{2v_r}{c}\right)kT_r + \left(\omega_{c0}\tau_0 - \frac{1}{2}\alpha\tau_0^2\right) \\ &= \omega_R t + \omega_D kT_r + \phi_0 \end{aligned} \quad (7)$$

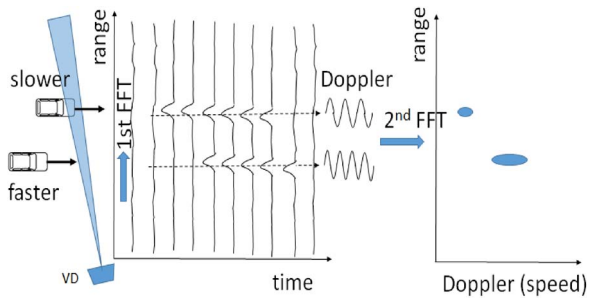

Fig. 4. Measurement scheme.

TABLE I
PARAMETERS USED IN SIMULATION

Parameters	Value
Center frequency	10.6 GHz
Sweep bandwidth	240 MHz
Sweep rate (PRF)	1000 Hz
Antenna beam width	9°
Antenna squint angle	10°
Range FFT length	512
Doppler FFT length	128

where the target frequency variables for the range and Doppler direction, i.e., ω_R and ω_D, respectively, are defined as

$$\omega_R = 2\omega_{c0}\frac{v_r}{c} + \alpha\tau_0 \quad (8)$$

$$\omega_D = 2\omega_{c0}\frac{v_r}{c}. \quad (9)$$

The FMCW measurement was periodically repeated, and a set of a number of N signals was recorded. Fig. 4 depicts the measurement scheme.

The complex analytic signal in (6) was used for the descriptions to simplify the following mathematical expressions:

$$s_b(t, kT_r) = A_b' \cdot e^{j(\omega_D \cdot kT_r + \omega_R \cdot t)}. \quad (10)$$

The complex amplitude A_b' comprises all constant phase terms. The 2-D FFT of this signal can be derived by applying the Fourier modulation theorem. With the spatial frequency variables r and v in the range and Doppler direction, the spectrum of $s_b(t, kT_r)$ is derived as

$$F\{s_b(t, kT_r)\} = S_b(r, v). \quad (11)$$

The VD procedure can be summarized as follows.

Step 1) *Estimate the range by applying the range FFT*: For each PRI, sample beat signals from the front end and obtain the beat frequency by applying FFT. The range is proportional to the frequency.

Step 2) *Estimate the dwell time of the vehicle in the sensing region*: An appropriate threshold must be set for a particular range bin.

Step 3) *Estimate vehicle speed v by applying the Doppler FFT*: At a particular range bin, sample range data from the first FFT and obtain the Doppler frequency by applying the second FFT.

Step 4) *Identify the vehicle length.*

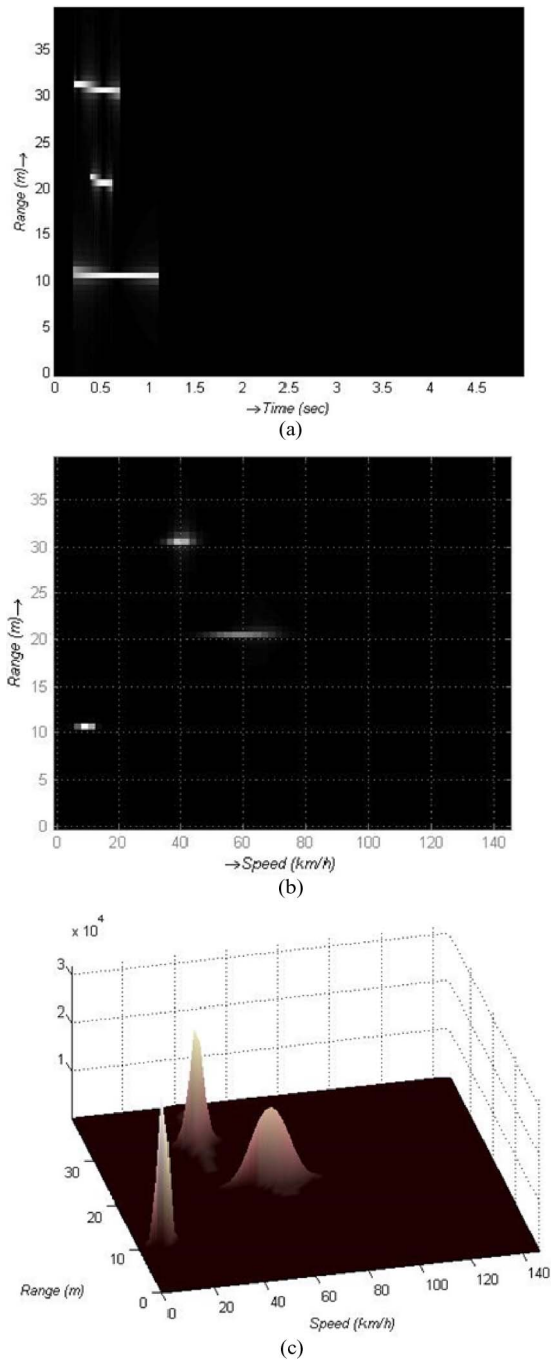

Fig. 5. Simulated 2-D spectrum of three moving vehicles. (a) Range spectra of three vehicles. (b) Range/speed spectra of three vehicles. (c) Range/speed spectra of three vehicles in 3-D.

The simulation used a data set for three vehicles simultaneously traveling distances of 10, 20, and 30 m through the detection zone at speeds of 10, 60, and 40 km/h, respectively. Table I shows the sensor parameters.

The target range and speed can be unambiguously determined by evaluating the positions of the three 2-D impulses based on (8) and (9). Fig. 5(a) shows that the range information for the vehicles was obtained by applying the range FFT for all sweep data. The speed information of each vehicle can be acquired during each CPI by applying a second FFT at each fixed range, because only one vehicle is at each fixed range.

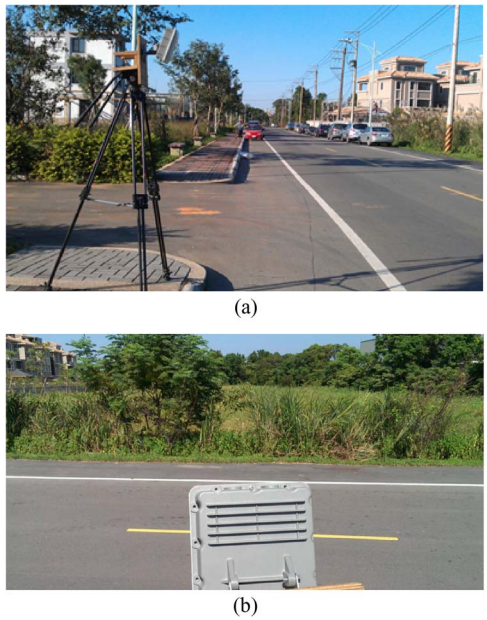

Fig. 6. VD setup. (a) VD setup at a height of 2 m and at a back-off distance of 3 m to the first lane. (b) VD setup with 10° squint angle.

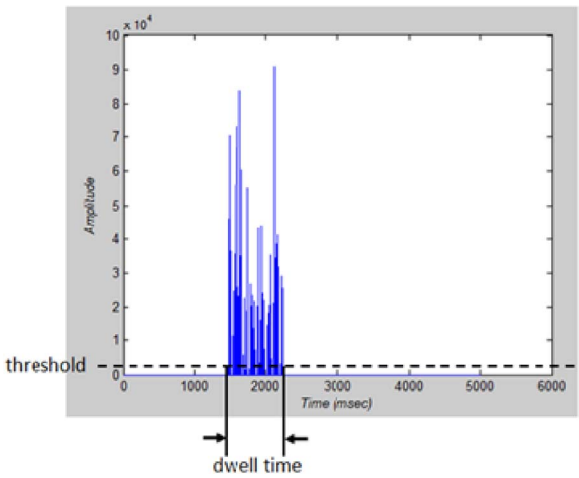

Fig. 7. Detected dwell time of a vehicle passing through the detection zone.

The speed measurement problem requires a peak search on the second FFT spectrum. By applying a single-tone frequency estimation method [16], the fine speed resolution can be obtained.

This method addresses several crucial issues. As shown in (8), the range response was shifted by the Doppler effects regarding the true position. However, the shifted range is substantially lower than the range resolution. The proposed approach requires a Doppler shift within the Nyquist limit determined by the PRF, i.e.,

$$\frac{-PRF}{2} < f_D < \frac{PRF}{2}$$

where

$$f_D = \frac{2v_r f_c}{c} = \frac{2v \cdot \sin(\theta) f_c}{c}. \tag{12}$$

The PRF must be sufficiently high to sample the instantaneous bandwidth. Equation (12) effectively controls the Doppler shift by adjusting the squint angle.

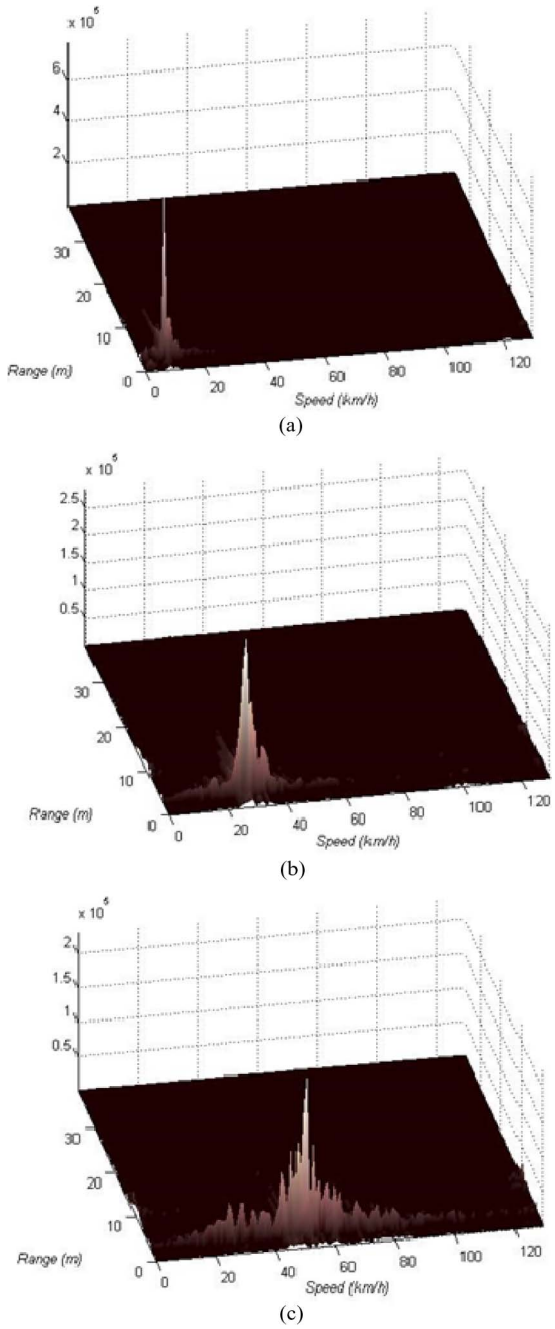

Fig. 8. Two-dimensional range/Doppler spectra measured at different speeds. (a) $v = 10$ km/h. (b) $v = 30$ km/h. (c) $v = 50$ km/h.

III. Experimental Results

This section presents experimental results to demonstrate the performance of the proposed method in side-looking speed measurement. The data were collected using a 10.6-GHz FMCW VD, as shown in Fig. 3. Fig. 6 shows the radar was mounted on a tripod beside the road at a height of 2 m and at a distance of 3 m to the first lane. Both lanes of the road were 3.5 m wide, and the radar beams were placed at a 10° squint angle facing the road. Table I shows the VD parameters. Because of the PRF limitations, the maximal unambiguous speed was 50 km/h. High performing hardware would be needed to measure higher speeds.

TABLE II
Measured Speed for Different Speeds at a Squint Angle of 10°

Test Items	Vehicle Speed (km/h)	Estimated Vehicle Speed (km/h)
1	10	10.1
2	20	22.4
3	30	30.5
4	40	39.7
5	50	54.0
6	-10	-11.9
7	-20	-22.0
8	-30	-25.8
9	-40	-41.7
10	-50	-52.9

Note: A positive value indicates a vehicle driving from left to right, and a negative value indicates a vehicle driving from right to left.

TABLE III
Estimated Vehicle Length for Various Speeds at a Squint Angle of 10°

Test Items	Vehicle Speed (km/h)	Dwell Time (ms)	Estimated Vehicle Length (m)
1	10	2025	4.8
2	20	1050	5.6
3	30	710	5.1
4	40	570	5.4
5	50	420	5.4
6	-10	1640	4.5
7	-20	1080	5.7
8	-30	770	4.6
9	-40	530	5.2
10	-50	425	5.3

The first test case confirmed that the 2-D FFT results enabled accurate speed measurements. The second test case further confirmed that the proposed method can simultaneously measure the speeds of multiple vehicles.

A. Test Case A: Various Speeds at a Squint Angle of 20°

The first experiment showed the ability of the proposed 2-D FFT approach to detect the speed and length of a vehicle. A vehicle with a length of 4.6 m was driven at speeds from 10 to 50 km/h in the first lane. The echo signal processed by the first FFT converts to range information. The dwell time for a vehicle in the detection zone can be measured by setting a suitable threshold at a specified range bin from consecutive frames. Fig. 7 shows the detected dwell time as the vehicle passed through the detection zone.

During the dwell period, the range FFT data of a target are collected for the Doppler spectrum after a second FFT. The Doppler spectra differ for various vehicle speeds. Fig. 8 shows that the 2-D range-Doppler spectra measured at various vehicle speeds had stronger peak signals at low speeds than at high speeds. These characteristics can solve the problem of imprecise speed measurement in most side-looking VD applications. Table II shows that the measurement error between actual and estimated speed was limited to ± 4 km/h.

From the measured dwell time and speed, the vehicle length can be derived using (1). The length must be calibrated by subtracting the beamwidth at Lane 1. Table III shows that the measurement error in the derived vehicle length at various speeds was limited to 1 m.

(a)

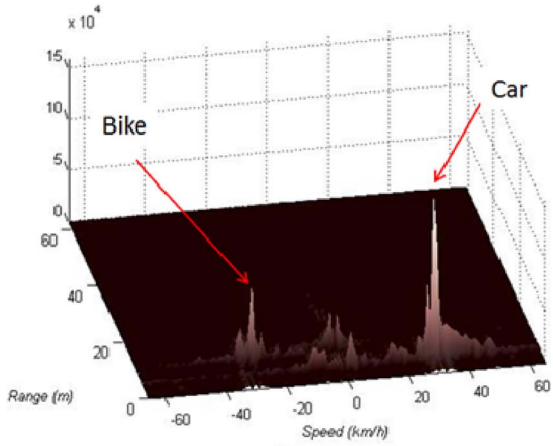

(b)

Fig. 9. Scenario of vehicles moving in opposite directions. (a) Snapshot of the scenario. (b) Range/speed spectrum.

B. Test Case B: Multiple-Target Detection

Three scenarios were used to demonstrate the effectiveness of the proposed method for simultaneous detection of multiple targets at various ranges and traveling at various speeds. The first scenario was two targets moving in opposite directions at approximately the same speed (30 km/h). Both moving objects encountered each other in the detection zone. Fig. 9(a) shows a photograph of the encounter. Although the echo power of the bike was lower than that of the car, Fig. 9(b) shows that both were distinguishable in the range-Doppler spectrum.

The second scenario was one car and one pedestrian moving in the same direction at low speeds. The spectrum in Fig. 10(b) shows that, although the pedestrian was walking at a slow speed (approximately 5 km/h), the echo power was sufficient for accurate detection. The third scenario was two small cars moving in the same direction at 15 km/h. Fig. 11(b) shows that the spectrum for this scenario had two distinguishable peaks.

Figs. 9–11 show that, although the return signals of farther objects were often partly obstructed by nearer objects, the proposed method correctly extracted the range and speed information. The proposed single-radar detection method accurately measured the speeds of slow-moving and obstructed objects even when power substantially differed between zones, which limits the accuracy of speed estimation in the dual-radar and multiple-zone approaches. The second advantage is that the speed coherent process in the second FFT accurately detects targets with a small radar cross section, i.e., vehicles, bikes, and pedestrians.

(a)

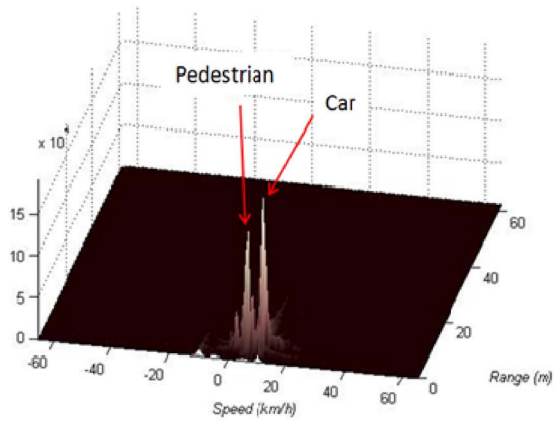

(b)

Fig. 10. Scenario of a car and a pedestrian moving in the same direction. (a) Snapshot of the scenario. (b) Range/speed spectrum.

(a)

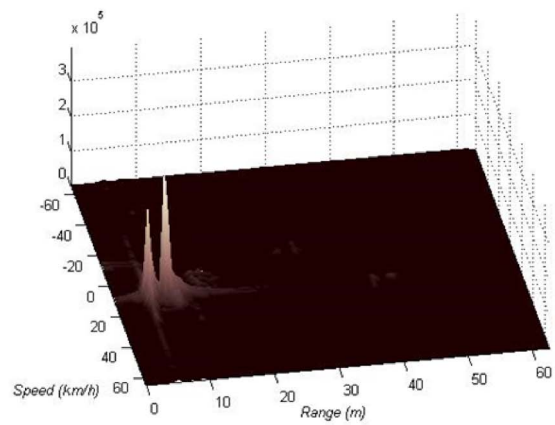

(b)

Fig. 11. Scenario of two cars moving in the same direction at 15 km/h. (a) Snapshot of the scenario. (b) Range/speed spectrum.

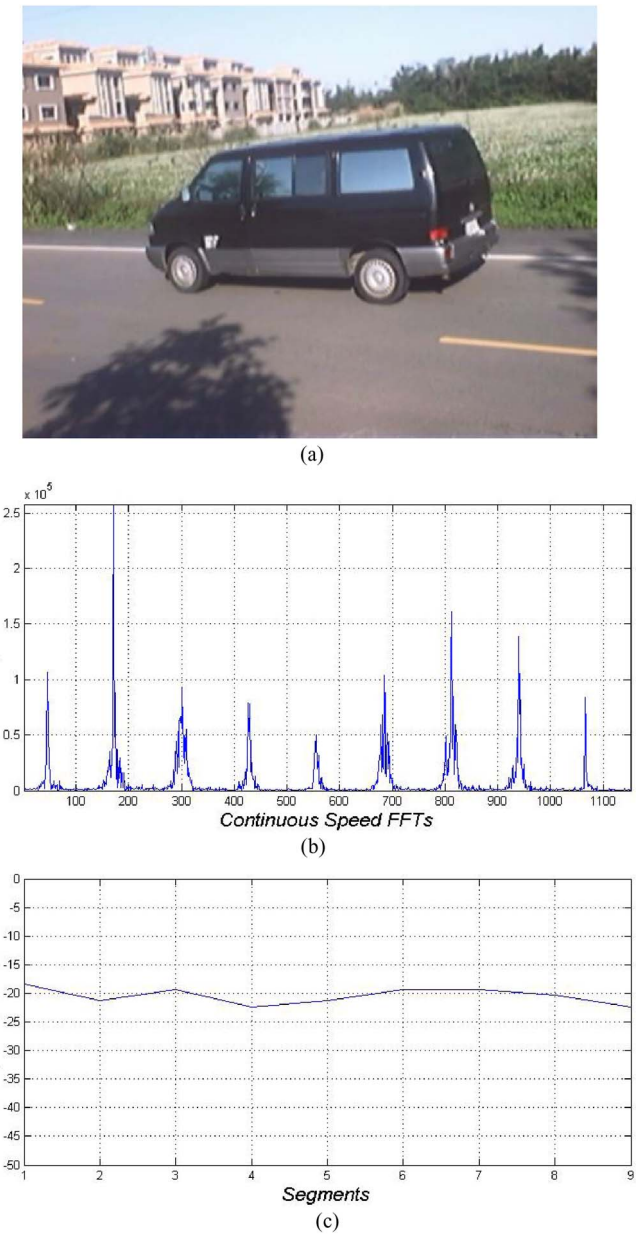

Fig. 12. Sequential Doppler spectra and tracked speed of a van traveling at 20 km/h. (a) Tested van. (b) Sequential Doppler spectra. (c) Tracked speed.

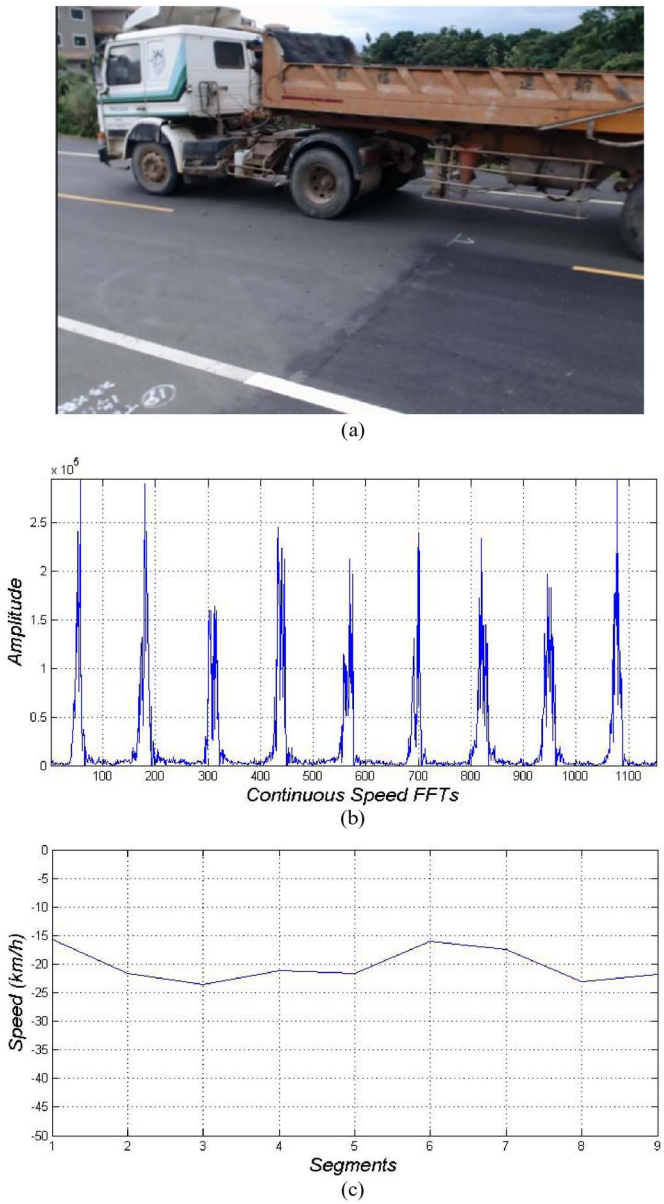

Fig. 13. Sequential Doppler spectra and tracked speed of a truck traveling at 20 km/h. (a) Tested truck. (b) Sequential Doppler spectra. (c) Tracked speed.

C. Test Case C: Signals for Different Vehicle Types

This experiment compared sequential 2-D FFT spectra between a van and a truck. The purpose of the experiment was to measure signal quality in a sequential 2-D FFT. The van (length, 4.9 m) and the truck (length, 12 m) were both driven at a constant speed (approximately 20 km/h). Fig. 12(b) shows that the 2-D FFT was applied to the signal for 1.152 s, which was the time when the van was in front of the sensing area. The 1152 sweeps obtained by the FFT at a 1-kHz sweep rate were equally divided into nine time sequences. Fig. 12(b) also shows the sequential results of Doppler spectra. Equation (12) was used to calculate the speed of the van based on the spectrum peak in each segment [see Fig. 12(c)]. The same procedure was used to derive the speed of the truck. Notably, the sharpness of the Doppler spectra in Fig. 13(b) is lower than that of the spectra in Fig. 12(b) because the wider Doppler bandwidth yielded a wider variation in speed estimates.

IV. Conclusion

Estimating and classifying vehicle speed are crucial problems in VDs used to gather traffic data in an ITS. However, as noted in Section I, per-vehicle speed estimation by side-looking single-beam microwave detection is generally inaccurate or unsupported. In addition, collecting reliable length data from these detectors is impossible because of the noisy speed estimates provided by conventional data aggregation for single-beam detectors.

The proposed algorithm enables accurate detection of per-vehicle speed and length by using side-looking single-beam microwave detectors. Unlike conventional side-looking radar sensors, the proposed method uses a squint angle to obtain

stronger Doppler signals compared with conventional sensors. Since the proposed scheme couples speed and range measurements for the lane in which a vehicle is moving, estimates of vehicle location and movement are unambiguous and reliable. The directions of moving vehicles are also determined according to negative- or positive-displacement Doppler shifts, regardless of the driving lane. The length of a vehicle can be also derived from its speed and the duration of time in the sensing zone. Therefore, a single radar can efficiently measure speed and monitor all lanes of a traffic route.

Simulations confirmed that the theoretical range-Doppler FMCW principle derived in this study can be used to detect multiple vehicles simultaneously. A commercially available 10.6-GHz radar and modified signal processing software were used for experimental tests. The experimental results show that the proposed algorithm is highly accurate, particularly at low speeds. The measurement error was less than 4 km/h. In addition to detecting vehicles, the experiments showed that the proposed method can detect weak moving targets, such as bikes and pedestrians.

Although the proposed algorithm exhibited acceptable performance at low speeds, further studies are needed to increase the applicable vehicle speed range for the algorithm. Reducing the squint angle can reduce radial speed but would also weaken the Doppler signal and speed resolution. The solution is using a DSP with higher performance capability to improve the robustness and accuracy of the proposed algorithm.

ACKNOWLEDGMENT

The authors would like to thank U&U Engineering, Inc. for supporting VDs and facilities to accomplish the experimental work and C.-M. Yang, H.-J. Hsu, and C.-Y. Hsu for implementing the experiments.

REFERENCES

[1] I. S. Kim, K. Jeong, and J. K. Jeong, "Two novel radar vehicle detectors for the replacement of a conventional loop detector," *Microw. J.*, vol. 44, no. 7, pp. 22–69, 2001.

[2] Y. H. Wang and N. L. Nihan, "Can single-loop detectors do the work of dual-loop detectors?" *J. Transp. Eng.*, vol. 129, no. 2, pp. 169–176, Mar. 2003.

[3] B. Coifman, S. Dhoorjaty, and Z. H. Lee, "Estimating median velocity instead of mean velocity at single loop detectors," *Transp. Res. C, Emerging Technol.*, vol. 11, no. 3/4, pp. 211–222, Jun.–Aug. 2003.

[4] B. Coifman and S. B. Kim, "Speed estimation and length based vehicle classification from freeway single-loop detectors," *Transp. Res. C, Emerging Technol.*, vol. 17, no. 4, pp. 349–364, Aug. 2009.

[5] S. J. Park, T. Y. Kim, S. M. Kang, and K. H. Koo, "A novel signal processing technique for vehicle detection radar," in *Proc. IEEE MTT-S Int. Microw. Symp. Dig.*, Philadelphia, PA, USA, Jun. 2003, vol. 1, pp. 607–610.

[6] P. J. Wang, C. M. Li, C. Y. Wu, and H. J. Li, "A channel awareness vehicle detector," *IEEE Trans. Intell. Transp. Syst.*, vol. 11, no. 2, pp. 339–347, Jun. 2010.

[7] H. Rohling, "Some radar topics: Waveform design, range CFAR AND target recognition," in *Advances in Sensing with Security Applications*. New York, NY, USA: Springer-Verlag, 2006, pp. 293–322.

[8] I. Urazghildiiev, R. Ragnarsson, and A. Rydberg, "High-resolution estimation of ranges using multiple-frequency CW radar," *IEEE Trans. Intell. Transp. Syst.*, vol. 8, no. 2, pp. 332–339, Jun. 2007.

[9] M. Skolnik, *Introduction to Radar Systems*., 3rd ed. Boston, MA, USA: McGraw-Hill, 2001.

[10] A. G. Stove, "Linear FMCW radar techniques," *Proc. Inst. Elect. Eng.–F, Radar Signal Process.*, vol. 139, no. 5, pp. 343–350, Oct. 1992.

[11] A. Wojtkiewicz, J. Misiurewicz, M. Nałecz, K. Jedrzejewski, and K. Kulpa, "Two-dimensional signal processing in FMCW radars," in *Proc. XX KKTOiUE*, Kołobrzeg, Poland, 1997, pp. 475–480.

[12] M. Vossiek, T. vonKerssenbrock, and P. Heide, "Signal processing methods for millimetrewave FMCW radar with high distance and Doppler resolution," in *Proc. 27th Eur. Microw. Conf.*, 1997, pp. 1127–1132.

[13] A. Meta, P. Hoogeboom, and L. P. Ligthart, "Signal processing for FMCW SAR," *IEEE Trans. Geosci. Remote Sens.*, vol. 45, no. 11, pp. 3519–3532, Nov. 2007.

[14] P. Marques and J. Dias, "Velocity estimation of fast moving targets using a single SAR sensor," *IEEE Trans. Aerosp. Electron. Syst.*, vol. 41, no. 1, pp. 75–89, Jan. 2005.

[15] N. Weber, S. Moedl, and M. Hackner, "A novel signal processing approach for microwave Doppler speed sensing," in *Proc. IEEE MTT-s Int. Microw. Symp.*, 2002, pp. 2233–2236.

[16] C. F. Huang, H. P. Lu, and W. H. Chieng, "Estimation of single-tone signal frequency with the special reference to frequency-modulated continuous wave system," *Meas. Sci. Technol.*, vol. 23, no. 3, pp. 35 002–35 012, Mar. 2012.

Shyr-Long Jeng was born in Taiwan in 1965. He received the Ph.D. degree in mechanical engineering from National Chiao Tung University, Hsinchu, Taiwan, in 1996.

From 1996 to 1998, he was with an electrical motor design company. He is currently an Associate Professor with the Department of Electrical and Electronic Engineering, Ta Hwa University of Science and Technology, Hsinchu. His research interest includes microprocessor-based control and applications.

Wei-Hua Chieng was born in Taiwan in 1959. He received the B.S. degree in mechanical engineering from National Tsing Hua University, Hsinchu, Taiwan, in 1982 and the M.S. degrees in mechanical engineering and in electrical engineering and the Ph.D. degree in mechanical engineering from Columbia University, New York, NY, USA, in 1986, 1987, and 1989, respectively.

From 1987 to 1989, he was awarded an IBM Manufacturing Fellowship. He is currently a Professor with the Department of Mechanical Engineering, National Chiao Tung University, Hsinchu. His research interests include automated control, mechatronics, and microelectromechanical systems.

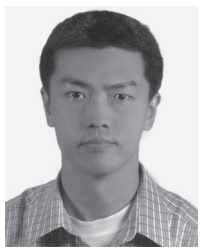

Hsiang-Pin Lu was born in Taiwan in 1966. He received the B.S. degree in computer science from Chung Cheng Institute of Technology, Taoyuan, Taiwan, in 1988 and the M.S. degree in computing from Imperial College London, London, U.K., in 1996.

He is currently a Research Assistant with National Chiao Tung University, Hsinchu, Taiwan. From 1988 to 2006, he was a Researcher with Chung-Shan Institute of Science and Technology, Taoyuan. His research interests include signal processing in frequency-modulated continuous-wave sensors, music cognition, and algorithmic composition.